Simulation of the physical process of neural electromagnetic signal generation based on a simple but functional bionic Na^+ channel

Fan Wang(王帆)[1,†], Jingjing Xu(徐晶晶)[1,2,†,‡], Yanbin Ge(葛彦斌)[1], Shengyong Xu(许胜勇)[3], Yanjun Fu(付琰军)[4], Caiyu Shi(石蔡语)[1], and Jianming Xue(薛建明)[4,§]

[1] *Institute of Microelectronics, Shandong University, Jinan* 250102, *China*
[2] *Shenzhen Research Institute of Shandong University, Shenzhen* 518057, *China*
[3] *Key Laboratory for the Physics & Chemistry of Nanodevices, and Department of Electronics, Peking University, Beijing* 100871, *China*
[4] *School of Physics, Peking University, Beijing* 100871, *China*

(Received 17 August 2021; revised manuscript received 18 October 2021; accepted manuscript online 24 November 2021)

The physical processes occurring at open Na^+ channels in neural fibers are essential for the understanding of the nature of neural signals and the mechanism by which the signals are generated and transmitted along nerves. However, there is a less generally accepted description of these physical processes. We studied changes in the transmembrane ionic flux and the resulting two types of electromagnetic signals by simulating the Na^+ transport across a bionic nanochannel model simplified from voltage-gated Na^+ channels. The results show that the Na^+ flux can reach a steady state in approximately 10 ns due to the dynamic equilibrium of the Na^+ ion concentration difference between both sides of the membrane. After characterizing the spectrum and transmission of these two electromagnetic signals, the low-frequency transmembrane electric field is regarded as the physical quantity transmitting in the waveguide-like lipid dielectric layer and triggering the neighboring voltage-gated channels. Factors influencing the Na^+ flux transport are also studied. The impact of the Na^+ concentration gradient is found to be higher than that of the initial transmembrane potential on the Na^+ transport rate, and introducing the surface-negative charge in the upper third channel could increase the transmembrane Na^+ current. This work can be further studied by improving the simulation model; however, the current work helps to better understand the electrical functions of voltage-gated ion channels in neural systems.

Keywords: neural signals, sodium-ion channel, transmembrane current, electromagnetic field

PACS: 87.19.L–, 87.16.Vy, 87.19.rp, 87.19.lq **DOI:** 10.1088/1674-1056/ac3cac

1. Introduction

In recent years, brain science has received increasing attention, and many countries have launched brain science research projects and made great progress in the field.[1–4] However, the basic question of how neural signals are transmitted and encoded in the nervous system remains very controversial. Several different hypotheses and models were proposed, including the cable model,[5,6] electromechanical soliton model,[7,8] electromagnetic field model,[9–11] quantum communication model[12] and quantum confinement superfluid model.[13] Their main differences lie in the physical nature of neural signals. The classic cable model described in textbooks considers these signals as the ionic current along the axons,[6] and this description has been widely debated.[7,14,15] Other models like the electromechanical soliton model and quantum confinement superfluid model claim that the neural signals act as mechanical waves.[7,8,13] The electromagnetic field model has demonstrated that the neural signals are electromagnetic signals originating from the transmembrane Na^+ flux across the ion channels.[11,12,16] The electromagnetic field model is the most popular view right now, although its description on the spectrum characteristics of the neural electromagnetic signals is unconvincing now. The key to making the physical nature of the neural electromagnetic signals clear lies in deciphering the generation processes of neural signals: that is, physical changes after opening the Na^+ or Ca^{2+} channels.

The Na^+ and Ca^{2+} channels across the membranes play the vital role in generating electromagnetic signals in the nervous, cardiovascular, and muscular systems.[17–19] These channels formed by proteins enable Na^+ or Ca^{2+} ions to pass across the membrane to generate nerve signals once activated by the local voltage change or other chemicals.[18] Here, the voltage-gated Na^+ channel is used as an example. The function and structure of the sodium-ion channels have been studied for nearly a century. In 1952, in the classic voltage-clamp experiment on squid axons, Hodgkin and Huxley found that changes in the permeability of a membrane to Na^+ and K^+ were the main source of action potentials. The Na^+ conductance of the cell membrane was found to determine the specific form of action potentials in nerves and muscles. Moreover, based on this, they proposed a mathematical model for activating and deactivating voltage-dependent channels.[6] In

[†]These authors contributed equally to this work.
[‡]Corresponding author. E-mail: xujj@sdu.edu.cn
[§]Corresponding author. E-mail: jmxue@pku.edu.cn

© 2022 Chinese Physical Society and IOP Publishing Ltd

CPB Online Express

1973, Keynes and Rojas studied the asymmetric displacement current in the giant axon of squid and concluded that this current was produced by the movement of the charge in the Na^+ channel gate system under the electric field; this movement of charge was called the gated current.[20] In the 1990s, the protein components of Na^+ channels were separated and purified, and more attention was paid to the association between voltage-dependent activation, inactivation, selectivity, and receptor sites in voltage-gated channels and their structures.[21,22] Recently, many researchers have committed to the study of the structure of activated Na^+ channels in cells and eukaryotes.[23,24] In 2017, Yan's group first reported the structure of Na^+ channels in electric eels' electroplax using a cryoelectron microscope.[25] Another study published in Cell in 2019 analyzed voltage-gated channels in bacteria and provided a reference for the structural study of Na^+ and Ca^{2+} channels in the resting state in eukaryotes.[26]

However, physical events during the open state of the channels have not been extensively studied. Information pertaining to these events can deepen our understanding of the generation of neural signals to determine the physical nature of neural electromagnetic signals, and provide us with clues to solve the mystery of the opening mechanism of voltage-gated channels. It can provide a solid reference for the transmission mechanism of electrical signals. To date, it is generally believed that voltage-gated Na^+ channels have a diameter of ~ 1 nm after being activated to open,[27] can remain open for approximately 100 μs–500 μs,[28,29] and the first half of the action potential (rising phase) mainly results from the opening of Na^+ channels.

Here, to study the spectrum characteristics of the neural electromagnetic signals, we constructed a bionic nanochannel to simulate physical events occurring after a Na^+ channel is opened. The events include the evolution of the ion concentration and transmembrane ionic current over time, as well as the changes induced in the transmembrane electric potential, electric field, and electromagnetic waves. We also discussed this influence of the process on the adjacent sodium-ion channels, thus providing a unique perspective on the in-depth understanding of voltage-gated ion channels and the neural signal transmission mechanism.

2. Materials and methods

2.1. Geometric model of the sodium-ion channel

The COMSOL Multiphysics 5.4 modeling system based on finite element analysis was selected to conduct most of this work. In view of the amount of calculation needed, in the present study, a bionic ion nanometer channel was simulated. As shown in Fig. 1, we constructed a geometric model of a Na^+ channel, where the length (l) and diameter (d) of the nanochannel were set as 10 nm and 1 nm, respectively.[27,30] The reservoirs above and below the channel had both a radius and height of 1 μm and were filled with high-concentration (150 mmol/L) and low-concentration (15 mmol/L) NaCl solutions, respectively.[18,31] The diffusion coefficient (D) of the Na^+ cation had a value of 2.46×10^{-9} m^2/s.[31]

As the Na^+ channels allowed Na^+ only to pass through, the bionic nanochannels should allow Na^+ to pass but prohibit anions from passing. Thin diffusion barrier layers with a thickness of 0.5 nm were therefore placed at both ends of the channel to achieve this. The diffusion coefficient of the Cl^- anion was then zero, whereas that of Na^+ was still D.

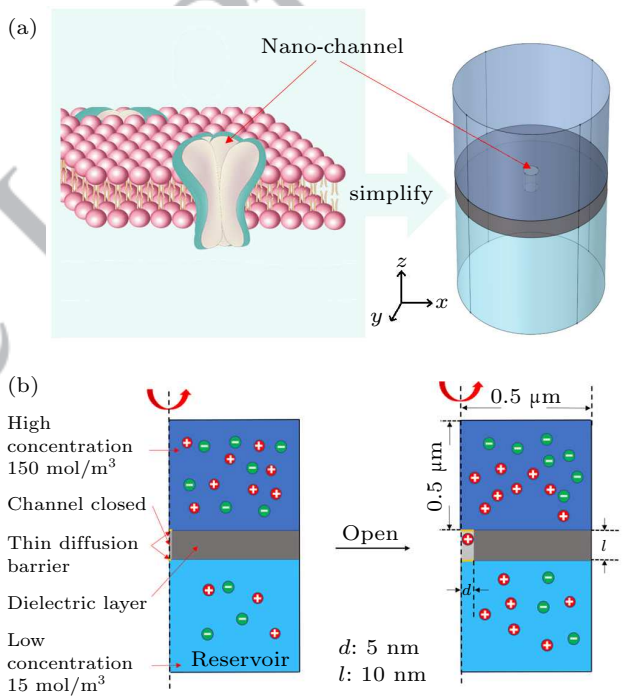


Fig. 1. A geometric model of the sodium-ion channel. (a) A diagram of transmembrane sodium channels and a simplified model of a channel. (b) The two-dimensional axisymmetric model used in the simulation with COMSOL Multiphysics 5.4.

2.2. Physical fields and boundary conditions

Considering the diffusion and migration of anions and cations in the biomimetic nanochannel under the concentration gradient, the transport of dilute species (TDS) module was selected to describe the diffusion and migration behavior described above. Simultaneously, a voltage of 70 mV between the areas of high and low Na^+ concentration was set across the dielectric layer to mimic the resting transmembrane potential in neurons. The electrostatic field module (ES) was then included to describe the influence of the transmembrane current and voltage on the transport of Na^+. The coupling parameter between the two physical fields (modules) — TDS and ES — was the electric potential (V).

The basic formulas and settings in the ES module include

the following:

$$\nabla \cdot D = \rho_{\rm v}, \tag{1}$$

$$E = -\nabla V, \tag{2}$$

$$\rho_{\rm v} = F \times \left(c_{\rm p} - c_{\rm n}\right), \tag{3}$$

where $\rho_{\rm v}$ is the net charge density in space and F is the Faraday constant. Here, $c_{\rm p}$ and $c_{\rm n}$ are the cation and anion concentrations, respectively.

The basic formulas and settings in the TDS module include the following:

$$\frac{\delta c_{\rm i}}{\delta t} + \nabla \cdot (-D_{\rm i}\nabla c_{\rm i} - z_{\rm i}\mu_{\rm m,i}Fc_{\rm i}\nabla V) + u\nabla c_{\rm i} = R_{\rm i}, \tag{4}$$

$$N_{\rm i} = -D_{\rm i}\nabla c_{\rm i} - z_{\rm i}\mu_{\rm m,i}Fc_{\rm i}\nabla V + uc_{\rm i}, \tag{5}$$

$$\mu_{\rm m,i} = D_{\rm i}/RT, \tag{6}$$

where $\mu_{\rm m,i}$ is the mobility, u is the flow velocity, $z_{\rm i}$ is the net number of charges, $c_{\rm i}$ is the ion concentration, and $D_{\rm i}$ is the diffusion coefficient of Na^+. Here, $R_{\rm i}$ and $N_{\rm i}$ represent the rate of change of the ion concentration and molar flux, respectively.

In the simulation, different grid sizes were used inside and outside the channel: the grid size inside the channel was set to 0.01 nm–1 nm, whereas the size outside the channel was set using the ultrafine grid in the software. The total number of grid cells used in the solution process was 2 million.

2.3. Calculation of transmembrane voltage/electric field and electromagnetic waves resulting from the transmembrane ionic current

By integrating the transmembrane ion current flux through the biomimetic nanochannel over time, the total charge transported from the area of high Na^+ concentration to that of low concentration under the ion concentration gradient and electrostatic field could be obtained as follows:

$$Q = \int I(t) \cdot {\rm d}t, \tag{7}$$

where $I(t)$ is the transmembrane ionic current, which is a function of time. Considering that the entire system — the dielectric layer and the solutions above and below this layer — constituted a biological capacitance,[32,33] the change in the transmembrane potential (ΔV) and electric field (ΔE) caused by the charge transport could be calculated using the following equations:

$$\Delta Q = \frac{1}{2}C_{\rm m}U^2, \tag{8}$$

$$\Delta E = \frac{\Delta V}{l}, \tag{9}$$

where $C_{\rm m}$ is the membrane capacitance, which had a value of 0.01 F/m^2,[34,35] and l is the length of the channel, which was also equal to the thickness of the dielectric layer (10 nm).

AnsysEM 19.2 was used to simulate the spectrum of electromagnetic fields induced by the ionic currents, and their electromagnetic distribution during transmission.

2.4. Validation of the settings used in the nanochannel model

After taking into account how the data were to be presented, the regions within 5 nm of the upper and lower ends of the channel were selected for observation. At the initial time ($t = 0$), the anion and cation concentrations inside the ion channel are both shown as zero, and the Na^+ concentrations in the upper and lower regions of the channel are 150 mM and 15 mM, respectively. At $t = 10$ ns, the distribution of the Na^+ concentration changes (Fig. 2(a)), whereas the concentration of Cl^- anions inside the channel remains zero (Fig. 2(b)) due to the existence of the thin diffusion barrier layer. These results confirm that the settings used for the initial boundary conditions and the use of the barrier layer were reasonable.

3. Results

3.1. Change in the distribution of the sodium-ion concentration and transmembrane ionic current

When activated, ion channels open, and Na^+ ions move from regions of high concentration to regions of low concentration, driven by both the concentration gradient and the transmembrane electric field. The Na^+ ions will redistribute themselves, thus affecting the subsequent transport of Na^+ ions. The simulated results for the Na^+ distribution show that the Na^+ concentration rapidly changes when the channel is opened and reaches equilibrium status within about 10 ns, producing a region where there is a slow and continuous decrease in concentration from high to low (see the inset in Fig. 2(a)). At the same time, the Cl^- distribution will tend to be dynamically stable, as shown in the enlarged part of Fig. 2(b). A dynamic change in the Na^+ concentration with time in the diametral plane was observed in the simulation. Figure 2(c) shows a graph of the distribution of the Na^+ concentration at dynamic equilibrium.

To gain a clearer understanding of the changes in the physical fields at different timescales after the opening of the sodium-ion channel, we simulated the channel current resulting from the transmembrane transport of Na^+ ions under the action of the concentration gradient and electrostatic field. The results are illustrated in Fig. 3(a), in which the inset is an enlarged detail showing the transmembrane ionic current during the first 50 ns of the simulation. The figure shows that after the opening of the channel, a peak current of 0.68 pA at $t = 2.5$ ns is produced due to the large concentration gradient between the two sides of the dielectric layer. Subsequently, the current rapidly drops to 0.45 pA within 10 ns–15 ns and remains at this level. This result is consistent with the condition that, after the channel is opened, the distribution of Na^+ rapidly reaches dynamic equilibrium.

CPB Online In Press

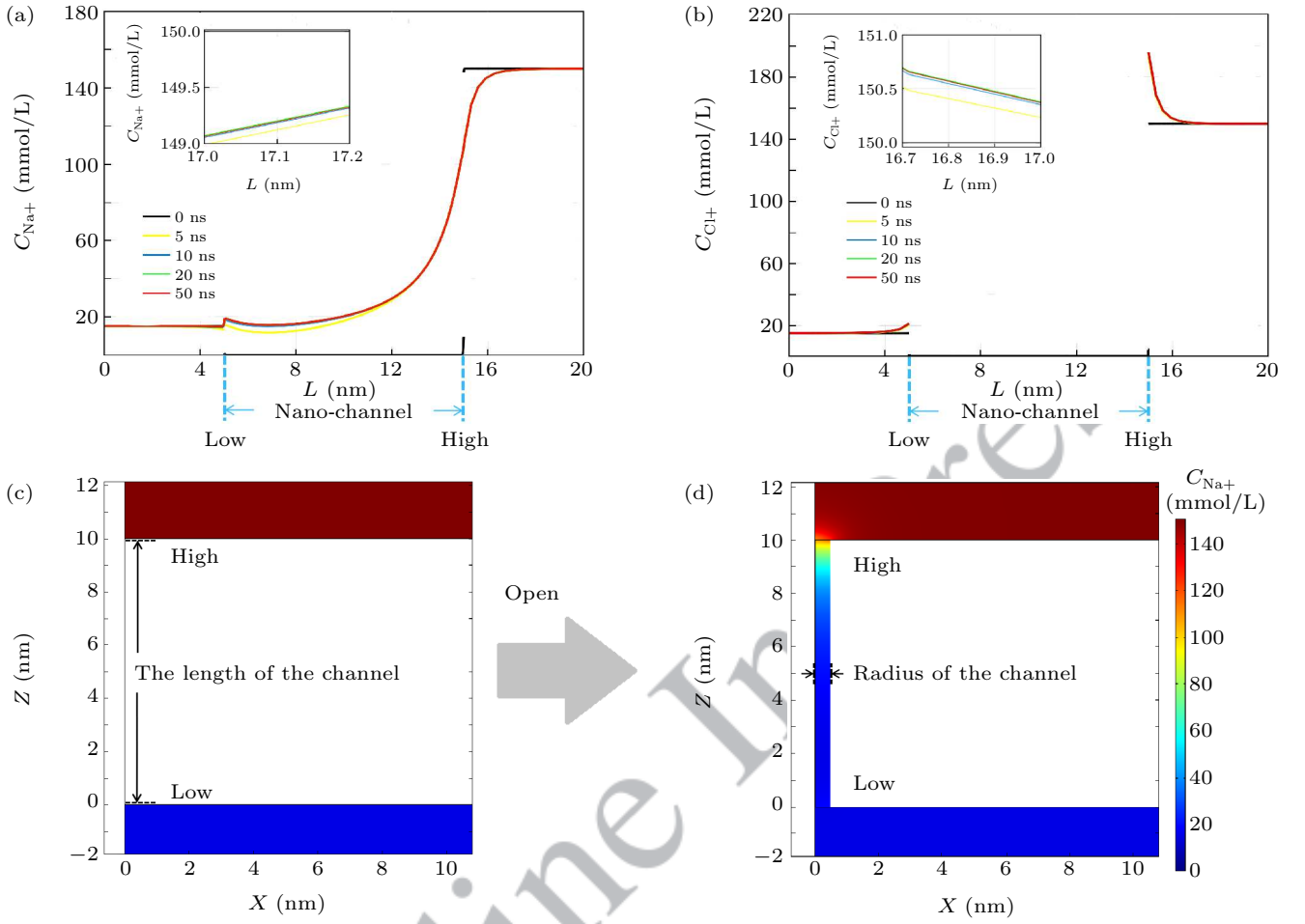


Fig. 2. The initial and later concentrations of (a) Na^+ and (b) Cl^- along the axis of the channel. The nanochannel was located between $L = 5$ nm and $L = 15$ nm. (c) The Na^+ concentration distribution at dynamic equilibrium.

3.2. The low-frequency electric field and high-frequency electromagnetic waves resulting from the transmembrane Na^+ flux

The redistribution of Na^+ ions leads to the changes in the transmembrane potential and transmembrane electric field, described using Eqs. (7)–(9). The results shown in Fig. 3(b) illustrate that the transmembrane voltage changes from the original value of −70 mV to −50 mV over a period of 50 μs after the nanochannel is opened, and then reaches +30 mV, equal to the action potential most frequently measured by electrophysiological instruments, at $t = 220$ μs. The increased transmembrane potential time is consistent with the reported open duration of Na^+ channels, i.e., 100 μs–500 μs.[28,29] As explained in detail in the discussion section, these two representative times are also consistent with many reported experimental results of the signal delay time.[15] The change in the transmembrane electric field change is illustrated in Fig. 3(b), where a rapid rate of change of 4.4×10^{10} V/(m·s) is shown.

According to Maxwell's equations,[36,37] this changing transmembrane current I in Fig. 3(a) generates two kinds of electromagnetic field signals. In the first 10 ns, the current changes rapidly and leads to a high-frequency electromagnetic wave. For the whole pulsed current within 0 μs–200 μs (taking 200 μs as the open time of nanochannels), it generates a low-frequency electromagnetic field. Using AnsysEM 19.2, the frequency spectra of these two signals are calculated. As shown in Fig. 3(c) and 3(d), the frequency ranges of two electromagnetic fields are 0.01 GHz–0.1 GHz and 0.001 MHz–1 MHz, respectively.

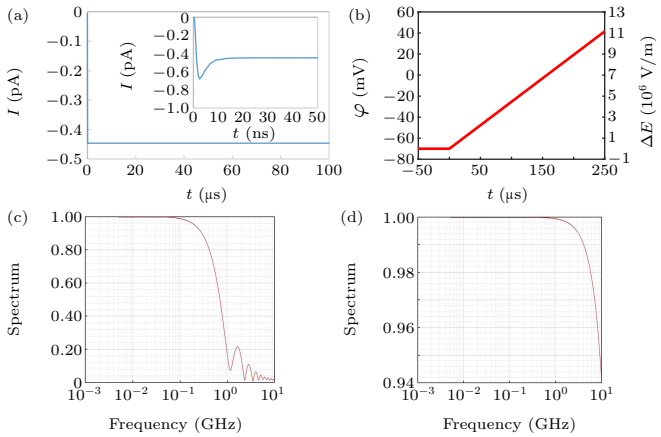


Fig. 3. The electromagnetic field change resulting from the Na^+ flux. (a) The transmembrane Na^+ current (I) passing through the nanochannel, (b) the resulting changes in the transmembrane potential (φ) and electric field (ΔE), (c) the spectrum distribution of the transmembrane current I in the first 10 ns, and (d) the spectrum distribution of the overall transmembrane current I (0 μm–200 μm).

CPB Online Ir

To thoroughly understand the electromagnetic field distribution and transmission of these two kinds of signals, an unmyelinated-axon model was constructed using a 10-nm thick cylindrical dielectric layer with NaCl solutions on both sides and an inner diameter of 1.14 μm in AnsysEM 19.2, as shown in Fig. 4(a). The relative dielectric constants of the dielectric layer and solution are considered to be 10.3 and 136, respectively, and their conductivities are 0 S/m and 1.454 S/m.[38,39] Eight current sources polarized in the radial direction are uniformly placed across the dielectric layer at the same cross-section to mimic the transmembrane ionic currents around axons, as shown in Fig. 4(b). Two sine currents corresponding to the transmembrane currents within two periods are chosen as the current sources to generate the stable electromagnetic field distribution. One current has an amplitude of 0.68 pA and a frequency of 50 MHz because of the half period of 10 ns, and the other has a peak value of 0.63 pA, i.e., the effective of 0.45 pA and the frequency of 2.5 kHz due to the half period of 200 μs. These two currents will generate two electromagnetic signals with the same frequency as them, respectively. Figure 4(c) illustrates the stable distribution of both the electric field and magnetic field of these two electromagnetic signals when they transmit 1 nm and 10 μm away.

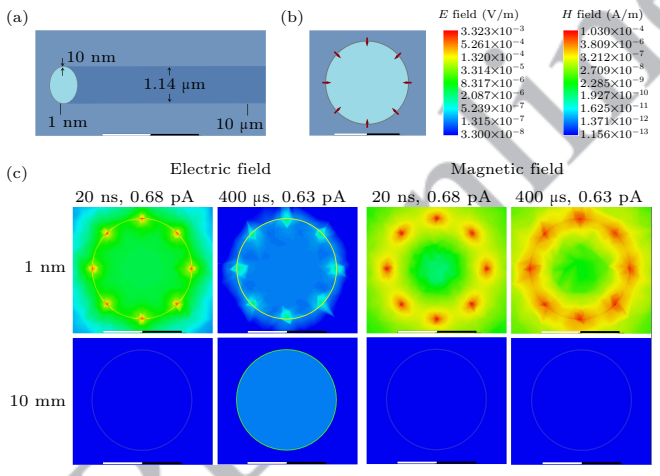


Fig. 4. Simulation of electromagnetic field distribution resulting from the two kinds of currents: (a) the applied unmyelinated axon model, (b) the setting of the eight currents, (c) the stable distribution of both the electric field and magnetic field of these two signals when they transmit 1 nm and 10 μm away.

Note that the electromagnetic fields, especially the electric field components, are mainly restricted in the dielectric layer under both conditions with different currents, supporting the point that the soft-material waveguide made of the dielectric layer and the solution on both sides contributes to the electromagnetic field transmission.[10,11,40] Furthermore, although its initial intensity is lower, the electric fields from the low-frequency signals (2.5 kHz) transmit more effectively in the dielectric layer compared with that from the high-frequency signals (50 MHz). This indicates that the low-frequency electromagnetic signals propagate better in the soft-material waveguides, consistent with reported findings.[11] For the high-frequency signals, the electric and magnetic fields attenuate to almost nothing at 10 μm away; thus it does not seem to be the high-frequency electromagnetic signals that transmit effectively in unmyelinated axons on which the distance between two adjacent channels is ∼ 10 μm.[18]

4. Discussion

4.1. Factors influencing the Na^+ flux through the nanochannel

The geometrical structure and physical properties of the channel and its surroundings can influence the Na^+ flux across the channel to adjust the formation of neural signals.

4.1.1. Concentration gradient and transmembrane potential

To explore the specific impacts of the main factors on the transmembrane ion current, we simulate the changes in the transmembrane current when the Na^+ concentration gradient across the dielectric layer and the initial transmembrane potential are reduced by 50%. The results are shown in Fig. 5(a). When the concentration gradient is reduced by half, the current decreases to 0.3 pA (gray line), with a drop of 33.3%. This drop percentage is very close to the previous electrophysiology experimental results of about 25% presented by Palmer *et al.* in 1998.[41] Conversely, the transmembrane current is reduced to 0.42 pA (orange line), which represents a decrease of 6.7% compared with the original current (blue line) when the transmembrane voltage decreases by 50%. However, we have not found a consistent relationship reported between the Na^+ current and the resting potential to evaluate the simulation results because of the interference of the clamping voltage.[42,43]

Our simulation results indicate that the change in the Na^+ concentration gradient has a significant effect on the Na^+ transport across the nanochannel, while the transmembrane potential has a relatively small impact. This result implies the importance of maintaining the surrounding solution environment, especially the concentration range and gradient of Na^+/Ca^{2+} for the normal discharge function of nerves. This is also believed to be in line with the self-protection principle in biological evolution: reducing the influence of external electromagnetic radiation on the functions of the nervous system.

4.1.2. Na^+ reservoir size

Meanwhile, the volume of the reservoir in the simulated model of the Na^+ channel is concluded to have an influence on the transmembrane current by influencing the Na^+ distribution change over time. Therefore, the transmembrane currents in the nanochannel with different-sized reservoirs are simulated, and the results are shown in Fig. 5(b). The transmembrane currents across the nanochannel with a Na^+ reservoir

Online-First Press

diameter of 0.03 μm–1 μm all reach the same stable value of 0.45 pA, although the Na^+ reservoir size can influence its early fluctuation. This diameter range corresponds to the density of the Na^+ channels in both the myelinated and unmyelinated nerves. In myelinated axons, the density of Na^+ channels at the Ranvier nodes has been reported to be 1000 μm^{-2},[11] implying that the average diameter of a reservoir for an individual channel is 30 nm (purple line), whereas it is approximately 0.3 μm (orange line) in unmyelinated axons, where the reported channel density is 10 μm^{-2}–15 μm^{-2}.[12,28] The density of Na^+ channels has almost no effect on low-frequency electric fields, but seems to be able to fine tune the intensity and spectrum of the high-frequency electromagnetic waves. For example, the intensity of a high-frequency electromagnetic wave in the nerve signal generated by a single Na^+ channel on an unmyelinated nerve seems slightly higher. Further research is needed to determine whether this phenomenon can regulate neurological function.

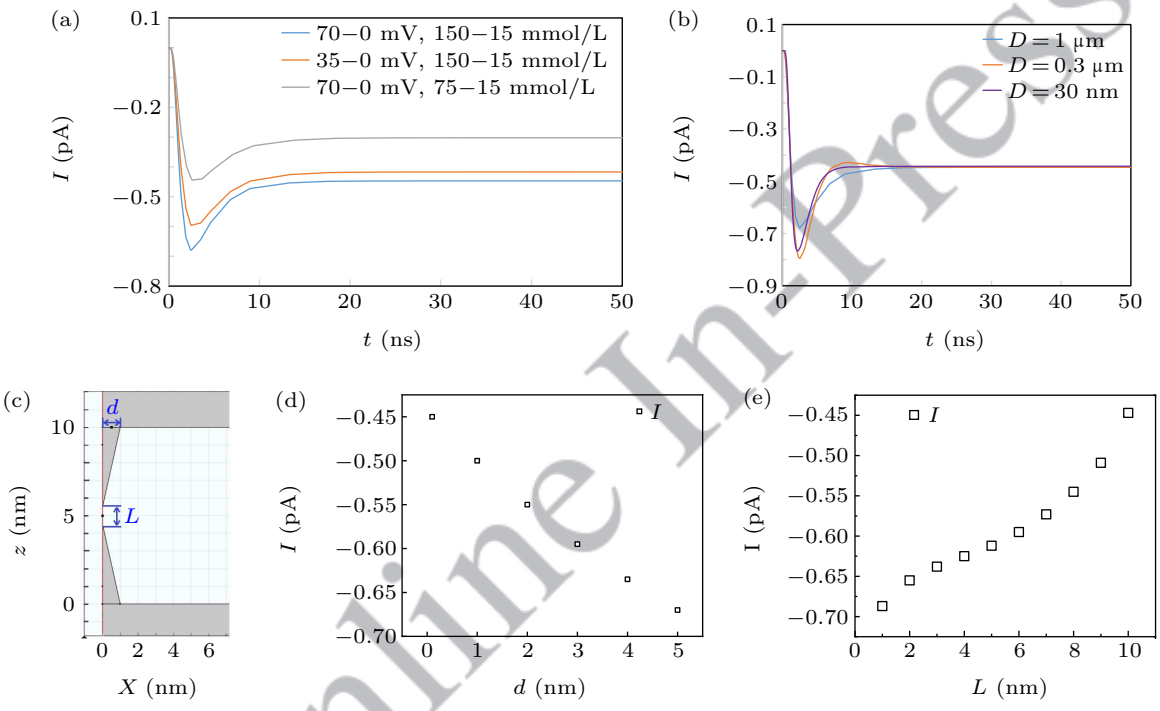


Fig. 5. (a) The influence of the Na^+ concentration gradient and initial transmembrane potential on the transmembrane current. (b) The effect of the reservoir volume on Na^+ transport across the nanochannel. (c) The effects of the geometry of the nanochannel.

4.1.3. Geometrical structure of channels

In some reported articles, voltage-gated Na^+ channels are described as being wide on both sides and narrow in the middle, similar to inverted funnels.[44] The transmembrane Na^+ current across this type of channel is related to the length of the narrowest channel, L, and the radius of the channel, d (Fig. 5(c)). Their effects, shown in Figs. 5(d) and 5(e), indicate that the ionic current is positively related to the radius of the channel with L of 1 nm, and negatively related to the length of the narrowest channel when d is fixed at 0.5 nm. Small changes in channel geometry have little effect on the stable value of the transmembrane ionic current.

4.1.4. Channel charge

The channel model here is designed to have the simplest form, considering that the physical process after the opening of Na^+ channels is the key issue in the generation of neural signals. However, there is no diffusion barrier layer for anions, as designed in the simple model of Na^+ channels in living organisms. It was reported that the filter group with negative charges in real Na^+ channels prevents the anions, such as Cl^-, from passing through channels.[25,44] To study the differences stemming from the structures of the model and the real channel, an improved model is constructed. In this model, the element of diffusion barrier layers is replaced with negative charges distributed on the inner surface of the upper third channel,[25] as shown in Fig. 6(a).

The simulation shows that the anion-blocking effect of the channel is related to the charge density. As shown in Fig. 6(b), the transmembrane current caused by Cl^- transport decreases with the charge density. When the surface charge density is set to -0.14877 e/nm^2, the transmembrane Cl^- current decreases to zero; this Na^+ channel model meets its biological function of selective permeability only for Na^+. In this model, the transmembrane ionic current (Fig. 6(c)) increases to a peak value of 8.88 pA at $t = 1.0$ ns and subsequently decreases to a stable value of 7.57 pA after 15 ns. Compared with the original simple model, this model provides higher current values but shows the same change trend in the current change over time.

CPB Online In Press

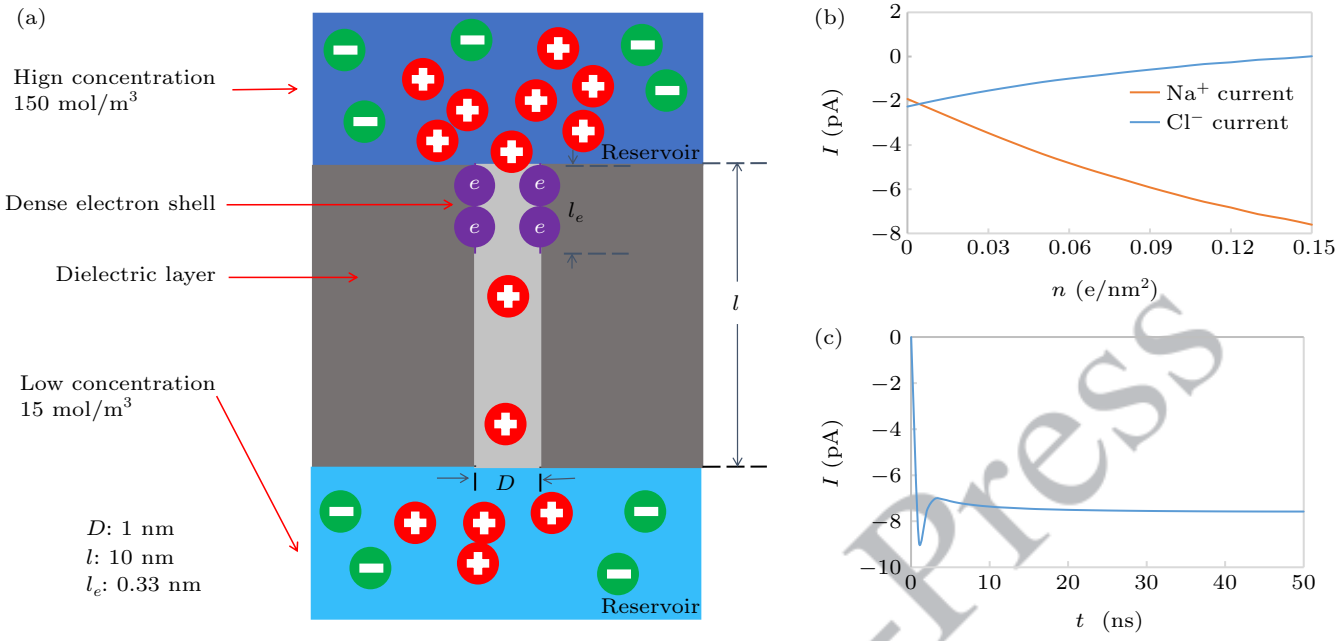


Fig. 6. Simulation results of the improved nanochannel model. (a) The improved model considering negative charges as the filter. (b) Currents from Cl^- anions and Na^+ cations versus negative charge density on the inner surface. (c) The transmembrane ionic current simulated in this model.

The introduction of negative charges in the channel can significantly facilitate the flow of Na^+ across the membrane. Correspondingly, the transmembrane voltage can reach up to +30 mV–+50 mV within approximately 20 μs: 10 times that in the original simple model. There are possible reasons for this difference. For example, the heterogeneity in the inner diameter of the Na^+ channel, where the diameter is less than 1 nm in some positions[25,44] and leads to a lower Na^+ transport speed, is ignored in the improved model. Consequently, we prefer the conjecture that for real sodium channels, the transmembrane current has a peak in the beginning 10 ns–15 ns and the value decreases and becomes stable, which corresponds to the stable values in the two models with 0.4 pA–2 pA, consistent with the reported values.[41,42,45] The previously reported increasing time of 100 μs[28,29] for the transmembrane potential from −70 mV to +30 mV is between these two simulation results, 20 μs from the improved model and 200 μs from the simple model. This is predictable, because the simulation models study the main variables, such as channel size, Na^+ selective permeability, Na^+ concentration, etc., ignoring some minor factors like the non-uniformity of the channel and the effects from other ions.

In summary, although the transmembrane Na^+ currents passing through the nanochannels change with some factors, such as the Na^+ concentration gradient, transmembrane potential, Na^+ reservoir size, geometrical structure and electrical properties of the channel, they have the same change trend, i.e., increasing to a peak about at $t = 1.0$ ns–2.5 ns and dropping back to a stable value within 10 ns–15 ns. As a result, the neural electromagnetic signals resulting from these transmembrane currents should have similar spatial-temporal and spectral characteristics to Figs. 3(c) and 3(d).

4.2. Possible activation mechanism of voltage-gated Na^+ channels

It is seen that the physical processes occurring after the Na^+ channel is activated mainly comprise the transmembrane ionic current, and the following high-frequency electromagnetic waves resulting from the rapidly changing current within the first 10 ns and the later low-frequency electric field, i.e., linear rapid change (4.4×10^{10} V/(m·s)) in the local transmembrane electric field. The viewpoint that the neural signals are high-frequency electromagnetic waves seems to be inconsistent with the simulation results in Fig. 4(c), where its electric and magnetic components both attenuate too much at 10 μm away to activate the neighboring Na^+ channels. The reported experimental results also disagree with the view, because of time mismatch. The delay time between two neighboring channel groups was reported as 10 μs–100 μs:[15] 3–4 orders higher than the total time of generation and transmission of the electromagnetic waves, 10 ns, considering its near-light-speed transmission. Consequently, the low-frequency transmembrane electric field is more likely to be the physical nature of neural signals.

In fact, the change in the transmembrane electric field occurs at the local channel as well as the neighboring channels due to the near-light-speed transmission of the field. Because of the waveguide structure made of lipid dielectrics, i.e., the membrane in unmyelinated axons or myelin sheath in myelinated axons, together with the intracellular and extracellular fluids, the change in the transmembrane electric field can be

CPB Online In-Press

transmitted more effectively than that in fluids, as explained using the electromagnetic field model.[10,11,46] As shown in Fig. 7, the local electric field variation at the first channels attenuates remarkably when arriving at the second channel ($t = 0$ μs). With time, the electric field variation around the second channel will increase to the threshold to activate the channel to open to generate a new neural signal ($t = 50$ μs).

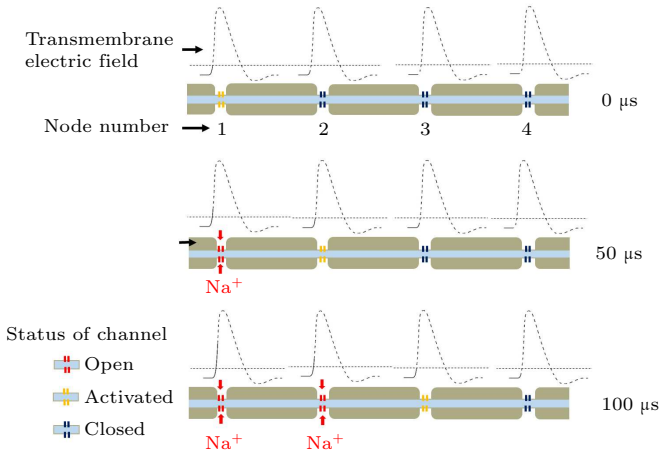


Fig. 7. The transmembrane electric field variation versus the status of the voltage-gated Na^+ channels.

This conclusion also provides clues for the understanding of the activation mechanism of voltage-gated ion channels. Currently, there are many models describing the activation of the channels, including the sliding helix,[47,48] paddle,[49,50] and transporter[51,52] models. Based on the above results and analysis, we propose that the physical factor activating the adjacent Na^+ channel is the low-frequency electric field perpendicular to the lipid membrane. We also derive a physical model for the voltage-gated Na^+ channel, which consists of an antenna-like charge group that can be displaced by changes in the local electric field to open the channel. A similar model was previously proposed.[53]

In this work, a simple bionic nanochannel model with continuous media is constructed to study the physical events and resulting neural electromagnetic signals after the channel is activated. Although there is scope to further improve the Na^+ channel model, the results presented here support the electromagnetic field model, in which the neural signals transmit in the form of the low-frequency transmembrane electric field which is perpendicular to the dielectric layer and propagates along the neural waveguide structure. In the future, the model could be improved to study more physical effects in detail in the generation process of neural signals.

5. Conclusion

We examined the transport of Na^+ across bionic nanochannels and the influencing factors and found the concentration gradient had a decisive impact on the transmembrane Na^+ current. The simulation results showed that the Na^+ distribution reached equilibrium within 10 ns after the channel was opened, leading to a high-frequency electromagnetic wave in 10 ns and a low-frequency transmembrane electric field in 200 μs. The result that the high-frequency electromagnetic wave was found to attenuate rapidly in transmission, together with the reported experimental phenomenon, showed that the low-frequency transmembrane electric field was considered as the neural electromagnetic signals which could propagate effectively in the waveguide-like structure. At last, an antenna-like activation mechanism may exist in the voltage-gated channels. Although the model developed in this study was simple and can be further improved, the findings of this study are still significant for understanding the generation and transmission mechanisms of neural signals in the nervous system and brain.

Acknowledgments

The authors are grateful to Prof. Mingzhi Li for valuable discussions. Project supported by the National Key Research and Development Program of China (Grant No. 2017YFA0701302), the Natural Science Foundation of Shandong Province, China (Grant No. ZR2020QA063), and Guangdong Basic and Applied Basic Research Foundation, China (Grant No. 2020A1515111180).

References

[1] Adams A, Albin S, Amunts K, Asakawa T and Zheng J 2020 *Neuron* **105** 947
[2] Amunts K, Ebell C, Muller J, Telefont M, Knoll A and Lippert T 2016 *Neuron* **92** 574
[3] Poo M M, Du J L, Ip N Y, Xiong Z Q, Xu B and Tan T 2016 *Neuron* **92** 591
[4] Martin C L and Chun M Y 2016 *Neuron* **92** 570
[5] Hodgkin A L and Huxley A F 1945 *J. Physiol-London.* **104** 176
[6] Hodgkin A L and Huxley A F 1952 *J. Physiol-London.* **117** 500
[7] Gonzalez-Perez A, Budvytyte R, Mosgaard L D, Nissen S and Heimburg T 2014 *Phys. Rev. X* **4** 031047
[8] Heimburg T and Jackson A D 2005 *Proc. Natl. Acad. Sci. USA* **102** 9790
[9] Xiang Z X, Tang C X, Chang C and Liu G Z 2021 *Nano Res.* **14** 590
[10] Xue J and Xu S 2012 *Quantitative Biology*
[11] Xu J J, Xu Y, Sun W, Li M and Xu S Y 2018 *Sci. Rep.* **8** 13824
[12] Hameroff S and Penrose R 2014 *Phys. Life Rev.* **11** 39
[13] Zhang X Q and Jiang L 2019 *Nano Res.* **12** 1219
[14] Bulai P M, Molchanov P G, Denisov A A, Pitlik T N and Cherenkevich S N 2012 *Eur. Biophys. J. Biophys. Lett.* **41** 319
[15] Xu J, Xu S J, Wang F and Xu S Y 2020 *Chin. Phys. B* **30** 028701
[16] Min Y, Kristiansen K, Boggs J M, Husted C, Zasadzinski J A and Israeiachvill J 2009 *Proc. Natl. Acad. Sci. USA* **106** 3154
[17] Chen K H S and Chen R 2020 *J. Mov. Disord.* **13** 27
[18] Bear M F, Connors B W and Paradiso M A 2007 *Neuroscience: Exploring the Brain*, 3rd Edition (Lippincott Williams & Wilkins)
[19] Finocchiaro G, Sheikh N, Biagini E, Papadakis M, Maurizi N, Sinagra G, Pelliccia A, Rapezzi C, Sharma S and Olivotto I 2020 *Heart Rhythm* **17** 142
[20] Keynes R D and Rojas E 1974 *J. Physiol-London.* **239** 393
[21] Guy H R and Conti F 1990 *Trends Neurosci.* **13** 201
[22] Lawrence J H, Tomaselli G F and Marban E 1993 *Heart Disease And Stroke: A Journal For Primary Care Physicians* **2** 75

CPB Online In-Press

[23] Shen H, Li Z, Jiang Y, Pan X, Wu J, Cristofori-Armstrong B, Smith J J, Chin Y K Y, Lei J, Zhou Q, King G F and Yan N 2018 *Science* **362** eaau2596

[24] Catterall W A, Wisedchaisri G and Zheng N 2017 *Nat. Chem. Biol.* **13** 455

[25] Shen H, Zhou Q, Pan X, Li Z, Wu J and Yan N 2017 *Science* **355** eaal4326

[26] Wisedchaisri G, Tonggu L, McCord E, El-Din T M G, Wang L, Zheng N and Catterall W A 2019 *Cell* **178** 993

[27] Lenaeus M J, Gamal ElDin T M, Ing C, Ramanadane K, R P, Zheng N and Catterall W A 2017 *Proc. Natl. Acad. Sci. USA* **114** E3051

[28] Edrich T, Wang S Y and Wang G K 2005 *J. Membr. Biol.* **207** 35

[29] Nelson P C 2013 *Biological Physics: Energy, Information, Life* (W.H. Freeman and Co)

[30] Pelttari A and Helminen H J 1979 *Histochem. J.* **11** 613

[31] Fu Y J, Guo X, Wang Y F, Wang X W and Xue J M 2019 *Nano Energy* **57** 783

[32] Yang F, Xu J J and Xu S Y 2016 *Neuroscience & Biomedical Engineering* **4** 230

[33] Xu J J, Wang F, Song Y H, Ge S and Xu S Y 2021 *IET Nanodielectrics* pp. 1–14

[34] Adelman W J 1969 *Electroencephalogr. Clin. Neurophysiol.* **27** 556

[35] Bertrand C A and Hopfer U 2002 *Methods Mol. Biol.* **188** 315

[36] Hammond P 1971 *Applied Electromagnetism* (Pergamon) p. 378

[37] Lawden D F 1973 *Electromagnetism* (George Allen & Unwin) p. 96

[38] Zhang L, Zhu X and Ni Z 2012 *J. Southeast Univ., Nat. Sci. Ed. (China)* **42** 280 (in Chinese)

[39] Niu Z Q 1994 *Chin. J. Biomed. Eng.* **13** 90 (in Chinese)

[40] Xu S Y 2017 *Med. Surgical. Ophthal. Res.* **1** 000501

[41] Lawrence G, Palmer, Henry, Sackin, Gustavo and Frindt 1998 *J. Physiol.* **509** 151

[42] Rosenberg R L, Tomiko S A and Agnew W S 1984 *Proc. Natl. Acad. Sci. U. S. A.* **81** 5594

[43] Filatov Gregory N, Pinter Martin J and Rich Mark M 2005 *J. Gen. Physiol* **126** 161

[44] McCusker E C, Bagneris C, Naylor C E, Cole A R, D'Avanzo N, Nichols C G and Wallace B A 2012 *Nat. Commun.* **3** 1102

[45] Palmer and L. G 1988 *J. Gen. Physiol* **92** 121

[46] Xu J J, Yang F, Han D H and Xu S Y 2018 *Biochem. Biophys. Res. Commun.* **496** 661

[47] Catterall and A W 1986 *Annu. Rev. Biochem.* **55** 953

[48] Catterall W A 1984 *Science* **223** 653

[49] Jiang Y X, Ruta V, Chen J Y, Lee A and MacKinnon R 2003 *Nature* **423** 42

[50] Jiang Y X, Lee A, Chen J Y, Ruta V, Cadene M, Chait B T and MacKinnon R 2003 *Nature* **423** 33

[51] Bezanilla F 2008 *Nat. Rev. Mol. Cell Biol.* **9** 323

[52] Batulan Z, Haddad G A and Blunck R 2010 *J. Biol. Chem.* **285** 14005

[53] Barber A F, Carnevale V, Raju S G, Amaral C, Treptow W and Klein M L 2012 *BBA-Biomembranes* **1818** 2120

CPB Online In Press